Bioelectrochemistry 94 (2013) 79–86

Contents lists available at ScienceDirect

Bioelectrochemistry

journal homepage: www.elsevier.com/locate/bioelechem

An experimental system for controlled exposure of biological samples to electrostatic discharges

Igor Marjanovič, Tadej Kotnik *

Department of Biomedical Engineering, Faculty of Electrical Engineering, University of Ljubljana, Tržaška 25, SI-1000 Ljubljana, Slovenia

ARTICLE INFO

Article history:
Received 18 July 2013
Received in revised form 2 September 2013
Accepted 2 September 2013
Available online 10 September 2013

Keywords:
Electrostatic discharge
Lightning
Electroporation
Gene electrotransfer
Exposure system

ABSTRACT

Electrostatic discharges occur naturally as lightning strokes, and artificially in light sources and in materials processing. When an electrostatic discharge interacts with living matter, the basic physical effects can be accompanied by biophysical and biochemical phenomena, including cell excitation, electroporation, and electrofusion. To study these phenomena, we developed an experimental system that provides easy sample insertion and removal, protection from airborne particles, observability during the experiment, accurate discharge origin positioning, discharge delivery into the sample either through an electric arc with adjustable air gap width or through direct contact, and reliable electrical insulation where required. We tested the system by assessing irreversible electroporation of *Escherichia coli* bacteria (15 mm discharge arc, 100 A peak current, 0.1 μs zero-to-peak time, 0.2 μs peak-to-halving time), and gene electrotransfer into CHO cells (7 mm discharge arc, 14 A peak current, 0.5 μs zero-to-peak time, 1.0 μs peak-to-halving time). Exposures to natural lightning stroke can also be studied with this system, as due to radial current dissipation, the conditions achieved by a stroke at a particular distance from its entry are also achieved by an artificial discharge with electric current downscaled in magnitude, but similar in time course, correspondingly closer to its entry.

1. Introduction

Electrostatic discharges have long been known to humans; in nature we encounter them in the form of atmospheric lightning strokes, while artificial electric arcs – the first one generated by Humphry Davy in 1809 [1] – have many fields of application, ranging from light sources (arc lamps, including fluorescent tubes) to a wide span of tools for processing of materials, particularly for welding, heating (arc furnaces) and plasma cutting. Recently, it was reported that nanosecond electric arcs (sparks) applied to living skin lead to a more efficient DNA uptake and expression than the standard approach in which electric pulses are delivered through electrodes in direct contact with the skin [2], and it was also suggested that lightning strokes could have contributed to DNA transfer during evolution [3–5].

The physics of the effects caused by electrostatic discharges interacting with simple materials is well understood. Most technological processes thus exploit the heat dissipated by the electric current of the arc (flowing either through the material or through the air nearby), while emission of light from arc lamps also involves ionization and quantum excitation of the gas through which this current flows. When flowing through a material, the electric current of the arc also induces an electric field in the material, which is the strongest at the current's point of entry, then gradually decreases as the current flow is dispersed over larger cross-sections inside the material, and – provided that its exit is also point-like – increases again to reach another peak at the point of exit.

When an electrostatic discharge interacts with living matter, the basic physical effects – the induced electric field, the temperature increase, and possibly ionization caused by the electric current – are the same as in simpler materials, but they can be accompanied by a range of biophysical and biochemical phenomena. Electric fields as weak as 60 mV/cm (for durations over 100 μs) excite nerve and muscle fibers, while much stronger fields (hundreds of V/cm or more) cause – in all cells, both excitable and non-excitable – a considerable increase of their membrane permeability (electroporation) and/or their merger (electrofusion). If the field is neither too strong nor too long-lasting, electroporation is reversible, while otherwise it becomes irreversible, resulting in cell death. With sufficient power dissipation, exposures to strong electric fields also cause thermal damage to the cell and its molecules (protein denaturation, DNA melting).

The phenomena of electroporation and electrofusion have been known for several decades. Electroporation was thus first reported for an excitable cell plasma membrane (Ranvier node of a myelinated axon) in 1958 [6], for a non-excitable cell plasma membrane (bacterial outer and cytoplasmic membrane) in 1967 [7], for organelle membrane (of a chromaffin granule) in 1972 [8], and for a planar lipid bilayer (oxidized cholesterol/n-decane) in 1979 [9]. Electrofusion was first demonstrated for animal cells (both anucleate and nucleated) in 1980, and for plant protoplasts and lipid vesicles in 1981 [10–13].

* Corresponding author. Tel.: +386 14 768 768; fax: +386 14 264 658.
E-mail address: tadej.kotnik@fe.uni-lj.si (T. Kotnik).

1567-5394/$ – see front matter © 2013 Elsevier B.V. All rights reserved.
http://dx.doi.org/10.1016/j.bioelechem.2013.09.001

Since their discovery, electroporation and electrofusion have been extensively investigated and have to date found multiple applications in medicine and biotechnology. In medicine, reversible electroporation is used for delivery of chemotherapeutics in cancer treatment [14] and of DNA in gene therapy [15], irreversible electroporation is a promising technique of tissue ablation [16], while electrofusion holds some promise in preparation of monoclonal antibodies for both diagnostics and therapeutics [17]. In biotechnology, irreversible electroporation is an efficient technique for extraction of biomolecules from cells and tissues [18,19], and is also useful – either accompanied by thermal effects or not – for inactivation or/and destruction of microorganisms [20].

Although some unknowns still remain, the physical properties of electroporation and electrofusion are by now generally well understood on the cellular and membrane level, while the recent molecular dynamics simulations are also improving our understanding of both phenomena on the molecular and atomic level [21–25]. Nevertheless, the mechanisms of electroporation-mediated transport, particularly of macromolecules such as DNA, are still a subject of vigorous investigation, as they likely involve several concurrent phenomena generated by the electric field pulses either directly (electroporation) or indirectly — by the resulting pressure waves (sonoporation) and/or thermal effects (thermoporation) [26,27].

Electroporation is, according to both theoretical considerations [28,29] and molecular dynamics simulations [22,23], an electric field-induced formation of aqueous pores in lipid parts of biological membranes. In this process, the water molecules penetrate into the lipid bilayer and interact there with adjacent membrane lipids that consequently reorient with their polar heads towards these water molecules, thus forming a polar pore wall. These pores render the membrane locally permeable to both ions and molecules. Electroporation occurs in the lipid bilayer of the membranes of all prokaryotic and eukaryotic cells, with the pores in the plasma membrane providing a pathway for transport of a wide range of molecules, including DNA, into [26] and out of the cell [7]. Pore formation is governed by electrochemistry and statistical thermodynamics [28,29] and due to the latter it is not strictly a threshold event, in the sense that the pores would only form in electric fields exceeding a certain level, but transport across the electroporated membrane is strongly correlated with transmembrane voltage induced by the electric field [30], which is in turn proportional to the strength of this field [30].

Electrofusion of two cells can occur both if they are in direct contact during the exposure to the electric pulses, or if they are brought into such contact within a sufficiently short time (seconds or even minutes) after the exposure [31,32]. Experiments also show that in electrofusion of two lipid bilayers, the monolayers in direct contact often fuse first, while the other two monolayers still appear intact [33]. This suggests that electrofusion proceeds in the same three stages broadly recognized in the physiological fusion of two cells in direct contact: first, their membranes' external monolayers, at least one of which is locally destabilized, fuse within the area containing the instability, forming a stalk; second, the fused monolayers move apart radially, forming a disk-shaped diaphragm and bringing the internal monolayers into contact; and finally, the rupture of the diaphragm creates a pore connecting the cytoplasms of the two cells, thus completing the fusion [34]. Physiological fusion and electrofusion then differ mainly in the trigger of local destabilization of the exterior monolayer that initiates the fusion — various fusogenic membrane proteins in the former case [35], and electric pulses in the latter [36].

In medical and biotechnological applications of electroporation and electrofusion, as well as in basic research of these phenomena and the accompanying thermal effects, the required electric fields are generated by a suitable voltage source and delivered through electrodes in direct contact with the sample. Furthermore, while the early voltage sources used for electroporation and electrofusion were based on a capacitor discharge and as such delivered exponentially decaying pulses, the modern sources largely deliver rectangular pulses, with the voltage turned on stepwise, sustained at a constant level for a preset duration of the pulse, and then turned off stepwise. Such a description is a slight idealization, but the rise- and falltimes of the commercially available rectangular pulse generators for electroporation are now well below a microsecond, and the variability of the pulse amplitude is in general within a few percent of the preset value. In this manner, the electrical parameters used for electroporation and/or electrofusion are well controlled, making the basic studies reproducible and the resulting applications reliable.

Electric fields with amplitudes and durations adequate for electroporation and electrofusion can also occur in natural environments when these are hit by a lightning stroke [4,5]. But unlike with the laboratory studies and applications of electroporation and electrofusion described above, a stroke proceeds through a highly conductive channel (electric arc) created by electrical breakdown of the air separating the cloud and the ground, and the time course of the electric current and the electric field induced by it as it flows through the ground are neither rectangular nor purely exponentially decaying. Furthermore, in the ground the current does not flow towards a well-defined electrode, but dissipates downward and outward from its point of entry, and consequently the amplitude of the electric field it induces decreases rapidly with increasing distance from this point.

To adequately study lightning-induced electroporation, electrofusion, and the accompanying physical, biophysical and biochemical effects, the standard equipment used in the studies and applications of electroporation and electrofusion would thus have to be adapted to reflect the abovementioned distinctions — the delivery of the electric current to the sample through an electric arc formed in the air, the current's roughly radial dissipation in the sample, and preferably also its specific time course.

In this article, we describe the design, construction and testing of a scalable modular exposure system built along the above-mentioned guidelines, allowing to expose samples of biological cells and tissues to an electrostatic discharge with an adjustable peak current (up to several hundred amperes) in a controlled environment (with a precisely defined arc length, and with monitored time course of the current flowing through the sample). This provides a reproducible emulation of a downscaled lightning stroke. The exposure system allows the researchers to incorporate the electrostatic discharge generator and the ground-simulating electrode(s) of their choice, to quickly adjust the arc length, and due to its modular nature the system also allows for quick assembly, disassembly, and thorough cleaning.

2. Materials and methods

2.1. System development

2.1.1. Computer modeling

The components of the exposure system and the construction of the system as a whole were first modeled computationally in SolidWorks 2013 (Dassault Systèmes SolidWorks Corporation, USA), which was used both for mechanical design and for material selection, with the latter also comprising a basic numerical assessment of the mechanical strength of the materials. For more advanced numerical calculations of lightning stroke simulations and electric field distribution within the exposed sample, we used COMSOL MultiPhysics 4.2 (Comsol, Stockholm, Sweden).

2.1.2. Materials

The main construction material was polyethylene plastic (PE 500 Natur, Simona AG, Germany), as it is a good electrical insulator, widely available, affordable, and easy to clean. To allow for visual monitoring of the sample during the experiment, transparent parts of the system were constructed from plexi-glass (PLEXIGLAS XT Tube Clear 0A070GT, Evonik Industries, Germany), which is also a good insulator and easy to clean. For the electrodes, we tested both copper and stainless steel,

opting for the latter in the final design, with the reasons for this choice described in Section 3.

2.1.3. Fabrication

All the components of the exposure system except for the electrostatic discharge generator were custom fabricated using CNC machinery (High-Z 720, CNC-STEP, Germany), routing bits (CMT Utensili, Italy) and universal router (F-900 A/G, Voestalpine, Austria). The reasons for custom fabrication were to construct an exposure system emulating as closely as reasonably achievable an actual lightning stroke, and to allow for modular assembly and simple disassembly of the components for cleaning and transportation.

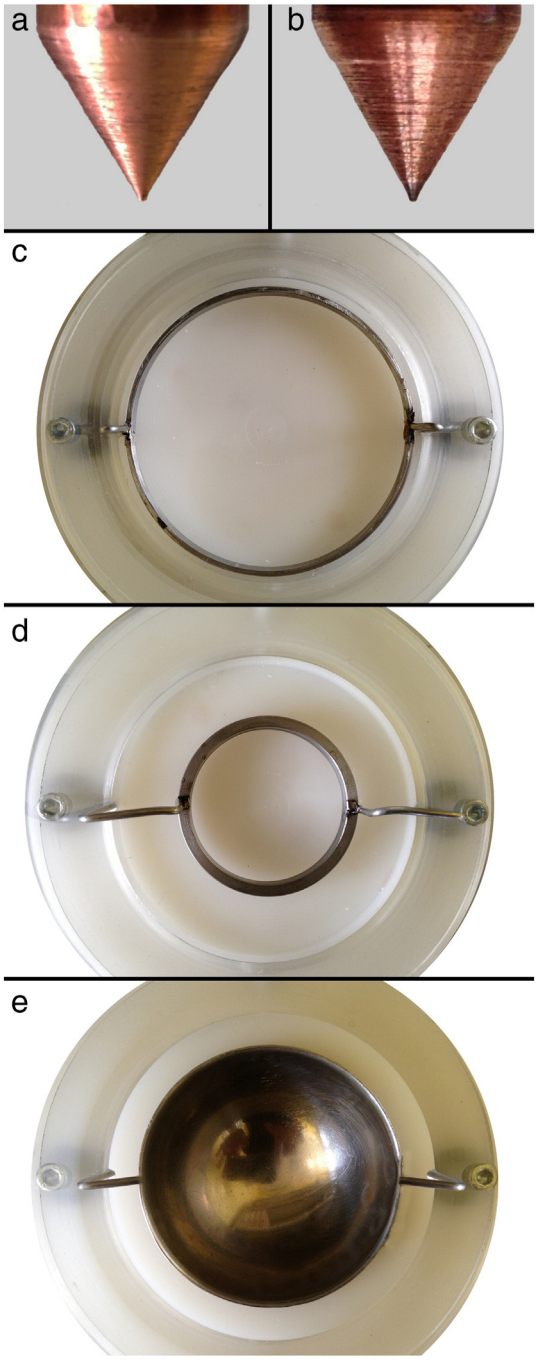

Fig. 1. (a–b) Corrosion of an emitting electrode made of copper. The electrode is shown before (a) and after (b) delivery of 500 discharges with approx. 100 A peak current, 0.1 μs zero-to-peak time, and 0.3 μs halving time into an agar plate. For an arc to form, the distance from the cone tip to the plate surface had to be gradually reduced from 15 mm for the first discharge to 11 mm for the 500th discharge. To avoid corrosion, we chose stainless steel for the final version of the emitting electrode. (c–e) Shapes of receiving electrodes made of stainless steel. (c) A ring electrode fitting into a 90 mm dish used for agar plating of bacteria. (d) A ring electrode fitting into a 60 mm dish for culturing of eukaryotic cells. (e) A hemispherical bucket electrode with an inner diameter of 70 mm suitable for three-dimensional cell populations growing in suspensions, gels, or soil, which are filled directly into the bucket. With a ring electrode the radial current dissipation is planar, while with the bucket electrode it is three-dimensional.

2.1.4. Discharge generator

Electrostatic discharges applied in our system testing (see Sections 2.2 and 2.3) were generated by commercially available taser gun (Great Power 750000, Great Power, South Korea). This device uses an amplifier circuit to amplify the source voltage, and an oscillator to generate the current that charges the capacitor connected to external electrodes; the capacitor discharges through these electrodes when the air breakdown voltage is reached between them, causing an electric arc across the air gap between the electrodes.

2.2. System testing on bacteria

2.2.1. Cultivation of Escherichia coli bacteria

E. coli K12 ER1821 strain (New England BioLabs, Frankfurt, Germany) was used as a model of bacterial cells. The cells were mixed with Luria broth (Sigma-Aldrich, Munich, Germany) in an Erlenmeyer flask and placed into an incubator with continuous shaking (I-50, Kambič Laboratory Equipment, Slovenia) for 24 h at 37 °C. After incubation, the flask was removed from the incubator and centrifuged for 15 min at 4 °C at 4200 RPM. Supernatant was then carefully removed, and pure water (Aqua B. Braun, Braun Melsungen, Germany) was added and stirred gently to suspend the cell pellet, and diluted further with additional pure water to a concentration of 5.5×10^8 CFU/ml to yield the final suspension of *E. coli*.

Agar plates were obtained by dissolving Luria agar (Sigma-Aldrich, Munich, Germany) in distilled water at 40 g/l, boiling for 15 min at 121 °C in an autoclave (A-11, Kambič Laboratory Equipment, Slovenia), cooling to 55 °C and spreading the solution uniformly in round Petri dishes with an inner diameter of 86 mm (90 mm Sterilin dishes, Thermo Scientific, UK) at 10 ml per dish. After the agar solidified and agar plates cooled to 21 °C, the final suspension of *E. coli* was poured uniformly over the surface of the plates at 1 ml per plate. After 1 min the suspension that did not get absorbed into agar was removed with a pipette. The agar plates were then left uncovered for additional 10 min in the laminar, allowing the remaining suspension to evaporate. At this stage there was no fluid present on the agar that would let bacterial cells to float and migrate. The electrical conductivity of the agar prepared in this manner was measured with LCR meter (Agilent 4284A Precision LCR Meter, Agilent Technologies, USA) at 1 MHz frequency and amounted to 22.9 mS/cm.

2.2.2. Irreversible electroporation

For electric discharge application, an agar plate with bacterial cells prepared as described above was loaded into the exposure system and 10 electric discharges were applied. The current of each discharge had a peak value of ~100 A, zero-to-peak time of ~0.1 μs, and halving time of ~0.3 μs, with the arc length of ~15 mm (see Fig. 5b). The control agar plate was loaded into the exposure system in the same manner as the exposed plates, but no discharge was applied. All plates were then incubated for 18 h at 37 °C.

2.2.3. Assessing the range of irreversible electroporation

After 18 h of post-exposure incubation, the top view of the agar plates was photographed using an 8-Mpixel digital video camera (iPhone 5, Apple, USA). The region of irreversible electroporation was clearly detectable as the central area with almost no colonies formed (see Fig. 3).

2.3. System testing on mammalian cells

2.3.1. Cultivation of CHO cells

Chinese Hamster Ovary cells (CHO-K1; European Collection of Cell Cultures, Great Britain) were used as a model of mammalian cells, plated in round Petri dishes with an inner diameter of 53 mm (60 mm TPP tissue culture dishes, Trasadingen, Switzerland) at 1.5×10^5 cells/ml. The culture medium consisted of F-12 HAM (Dulbecco's modification of Eagle's Minimum Essential Medium; Sigma-Aldrich Chemie, Deisenhofen, Germany) supplemented with 10% fetal bovine serum and 0.15 mg/ml L-glutamine (both Sigma-Aldrich Chemie, Deisenhofen, Germany). The electrical conductivity of the culture medium was measured with LCR meter (Agilent 4284A Precision LCR Meter, Agilent Technologies, USA) at 1 MHz frequency and amounted to 14.9 mS/cm.

Before exposure to electric discharges, the Petri dishes were kept in an incubator (I-CO2-235, Kambič Laboratory Equipment, Slovenia) at 37 °C and 5% CO_2 for 24 h, yielding approximately 4×10^5 cells per dish in exponential growth phase at the time of exposure.

2.3.2. Gene electrotransfer

Before electric discharge application, the culture medium was removed from the Petri dishes and replaced in each dish by 1.5 ml of fresh culture medium containing 4 μg/ml of pEGFP-N1 plasmid DNA (Clontech, USA; 4649 base pairs), which expresses green fluorescent protein (GFP, excitation 488 nm, emission 520 nm). After 2–3 min of incubation at 21 °C, a Petri dish was loaded into our exposure system and 10 electric discharges were applied. The current of each discharge had a peak value of ~14 A, zero-to-peak time of ~0.5 μs, and halving time of ~1.5 μs, with the arc length of ~7 mm. The control dish was loaded into the exposure system in the same manner as the exposed dishes, but no discharge was applied. After the exposure, the Petri dishes were incubated at 37 °C and 5% CO_2 for 5 min, then 3.5 ml of culture medium was added per dish, and all dishes were incubated for 24 h at 37 °C and 5% CO_2.

2.3.3. Assessing the fraction of electrotransfected cells

After 24 h of post-exposure incubation, the expression of GFP was assessed by observing the cells under an inverted fluorescence microscope (Axiovert 200, Zeiss, Germany) at 100× magnification. The fluorescence images were taken along a band 46 mm long and 0.7 mm wide passing through the center of the Petri dish, yielding 75 contiguous microphotograph frames. The number of transfected cells (those expressing GFP) per frame was estimated by counting the cells emitting clearly detectable fluorescence at 520 nm (see Fig. 4).

3. Results and discussion

3.1. System development

3.1.1. Emitting electrode design

The emitting electrode was shaped conically, with the cone tip pointing vertically downward. This provides a precisely defined position of the origin of electric discharge with respect to the sample positioned below, and a controlled distance from the cone tip to the sample surface, with the electric arc formed in the air separating them.

Our first prototype emitting electrode was made of copper, but the experiments showed that discharges delivered from this electrode caused its oxidation. This effect was progressive and most pronounced at the very tip of the cone (Fig. 1a–b), with the resulting layer of copper oxide gradually reducing the electrical conductivity of the cone, thereby affecting the peak current and the typical shape of discharges generated in an otherwise fixed setup. The initial properties of the emitting electrode were restorable by removing the oxide layer with a fine sandpaper, but due to the unpredictability and poor reproducibility of arcs generated using this electrode we abandoned it.

The final emitting electrode was therefore made of stainless steel. While copper has a higher electrical conductivity (5.9×10^5 S/cm at 20 °C) than stainless steel (1.4×10^4 S/cm at 20 °C), the resistivity of an electrode made from either material is very low compared to that of aqueous solutions (physiological saline has an electrical conductivity

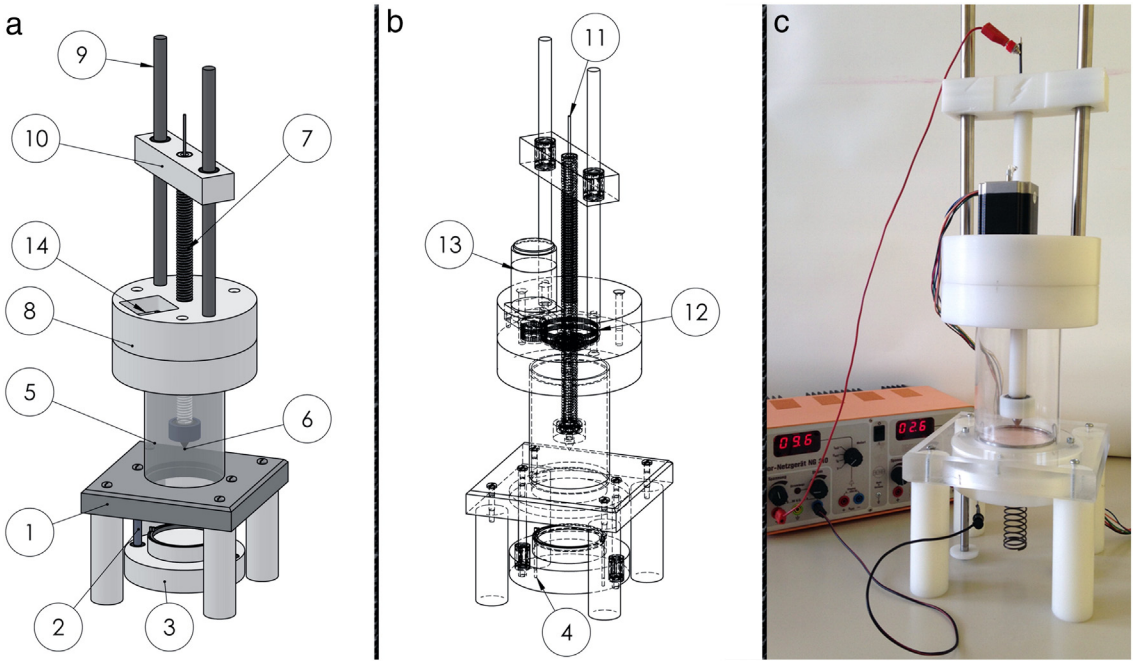

Fig. 2. The exposure system. (a–b) Major components in solid (a) and wireframe (b) representation: (1) base, (2) dock guide, (3) sample loading dock, (4) receiving electrode connector, (5) transparent tube container, (6) emitting electrode tip, (7) emitting electrode encasement, (8) core, (9) emitting electrode guide, (10) upper stabilizer, (11) emitting electrode connector, (12) central cogwheel, (13) stepper motor with its cogwheel, (14) stepper motor slot. (c) The actual prototype with a Petri dish in the loading dock locked in its upper position, a stepper motor in the core, and connected to a voltage generator.

of 12 mS/cm at 20 °C), and negligible compared to the resistivity of air. Thus, a change of emitting electrode material from copper to stainless steel had no detectable effect on the peak and time course of the electric current generated by the same arc-forming circuit. On the other hand, the stainless-steel emitting electrode proved much more resistant to discharge-induced corrosion, with thousands of reproducible consecutive discharges. In addition, stainless steel electrodes are also much more resistant to water-induced corrosion than copper electrodes, so they can also be washed with detergents if required.

3.1.2. Receiving electrode design

The receiving electrode was designed as to be in direct contact with a sample. Therefore, stainless steel was chosen as the construction material, as it is resistant to corrosion and dissolution in aqueous environments, nontoxic for biological samples, and easy to clean. To ensure a radial dissipation of the electric current from its point of entry into the sample, the receiving electrode was shaped either as a ring fitting inside the inner radius of a dish, ensuring two-dimensional current dissipation (Fig. 1c–d), or as a bucket shaped as a hemispherical shell, ensuring three-dimensional dissipation (Fig. 1e). In the former case, the dish is filled with the biological sample, while in the latter, the bucket electrode itself serves as a container.

3.1.3. Exposure system design

With the overall design of the exposure system, we tried to meet the following requirements:

- easy insertion and removal of a sample,
- protection of the sample from airborne particles (dust, microorganisms, etc.),
- observability of the sample during the experiment,
- easy connection of the discharge generator,
- easy and accurate adjustment of the emitting electrode vertical position,
- reliable electrical insulation where required.

The system consists of fourteen major components as shown in Fig. 2. The relatively broad and heavy base provides a low center of system's mass, ensuring its stability. Attached to the base via two guides is the sample loading dock with the receiving electrode. The loading dock is moved vertically along the guides, with its lower position (Fig. 2a–b) allowing for easy sample loading as well as unloading, and its upper position (Fig. 2c) magnetically locked, so that the dock with the loaded sample forms the bottom of the hollow and transparent tube container. The conical tip of the emitting electrode approaches the sample from above within the tube container, with the cylindrical body of the electrode and its electrically insulating encasement protruding vertically upwards through the core. The electrode body has a 1.2-mm radius, while its encasement consists, concentrically outwards, of a 0.3-mm layer of polyvinyl chloride and a 6-mm layer of polyethylene, which prevents dielectric breakdown for delivered voltages up to at least 120 kV (even if such a voltage was sustained indefinitely).

Above the core, the electrode body and its encasement run in parallel with two guides, proceeding to and through the upper stabilizer, above which the emitting electrode has its connector. The upper stabilizer slides along the guides, while the electrode encasement is fixed to the stabilizer. The encasement is threaded, and the base contains a central cogwheel with a matching inner threading, so that the cogwheel's rotation causes vertical movement of the encasement and the electrode inside it. For automated adjustment of the vertical position of the emitting electrode tip, the central cogwheel can also be rotated by a stepper motor with a suitable cogwheel transmission, and the core provides a slot for such a motor.

In our system, the non-transparent electrically insulating parts (base legs, loading dock, core, emitting electrode encasement, upper stabilizer) were made of polyethylene plastic, and the transparent parts (base platform, tube container) of plexi-glass. The electrodes and the guides were made of stainless steel.

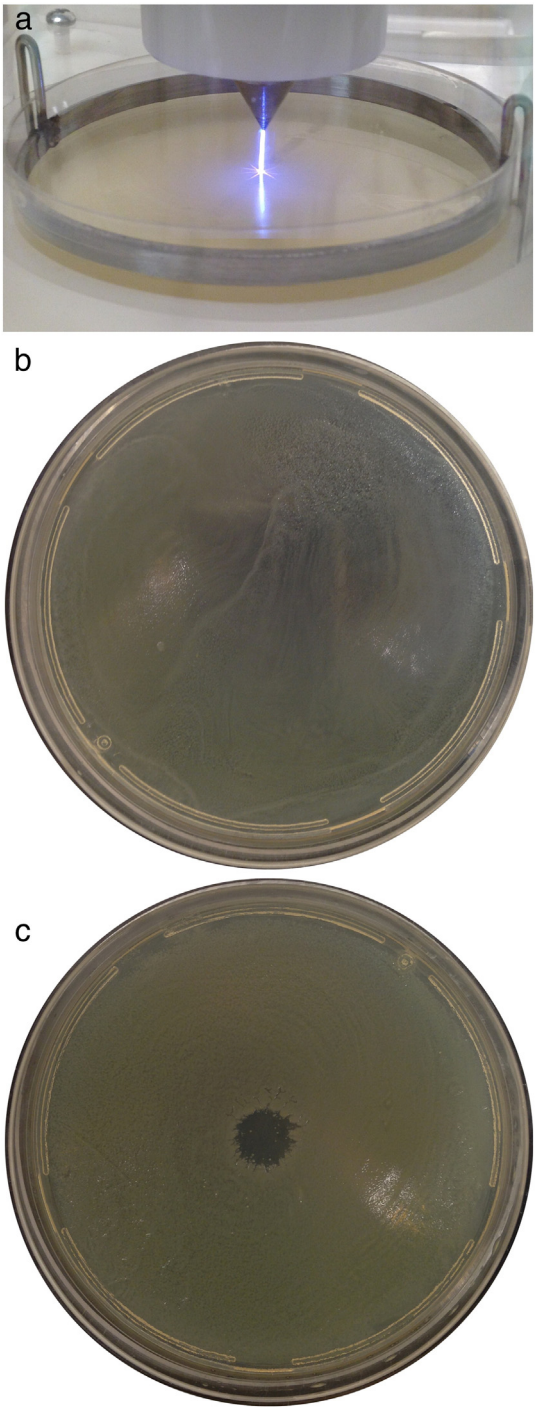

Fig. 3. Irreversible electroporation of *E. coli* with ten discharges of approx. 100 A peak current (for other parameter values, see main text). (a) The exposure. (b) The control plate (loaded into the system, but no discharge applied). (c) The exposed plate. The transparent areas correspond to regions with absence of *E. coli* colonies.

3.2. System testing

To test our exposure system, we performed two experiments. In the first experiment, we assessed irreversible electroporation of *E. coli* bacteria, while in the second experiment, we evaluated the fraction of electrotransfected CHO cells.

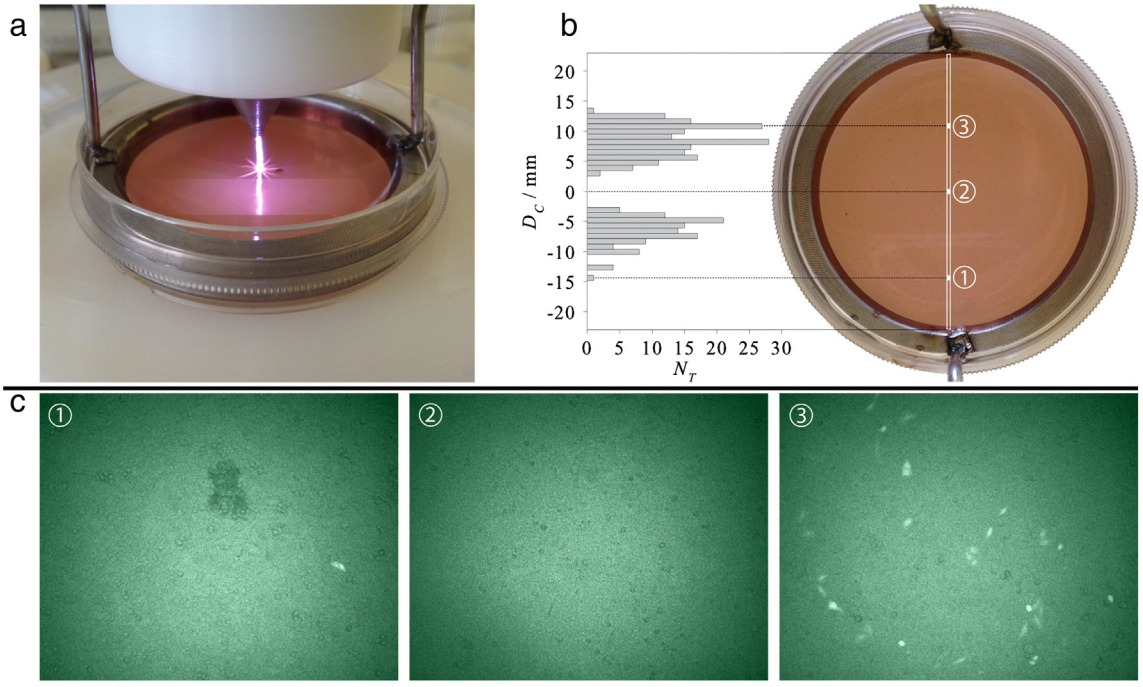

Fig. 4. Gene electrotransfer into CHO cells with ten discharges of approx. 14 A peak current (for other parameter values, see main text). (a) The exposure. (b) The exposed dish and the number of transfected cells per frame (N_T) as a function of the distance from the center of the Petri dish (D_C), counted along a band 46 mm long and 0.7 mm wide passing through the center of the dish. (c) Three microphotograph frames of the fluorescence emitted at 520 nm, indicating the transfected cells (location of these frames within the band is marked in the top right view of the dish).

3.2.1. Irreversible electroporation of bacteria

Fig. 3 shows the effect of ten discharges with a peak current value of 97(±8) A, zero-to-peak time of 0.11(±0.01) μs, peak-to-halving time of 0.17(±0.03) μs, arc length of 15.0 mm, and 29(±2) ms delay between consecutive discharges, on the colony forming ability of *E. coli* bacteria in a 90 mm agar plate. The receiving ring electrode had an outer diameter of 86 mm (fitting closely to the inner side of the plate wall) and an inner diameter of 82 mm.

As the figure shows, this exposure resulted in a central area of approximately 5 mm radius almost devoid of *E. coli* colonies. For a radial dissipation of electric current $I = 100$ A through a planar agar layer with thickness $d = 1.72$ mm (10 ml of agar spread across a disk with an 86 mm diameter), the electric current density at a distance $r = 5$ mm from the center can be estimated as

$$J \approx I/(2\pi r d) \approx 185\,\mathrm{A/cm^2}, \quad (1)$$

and the electric field it induces in a medium with electrical conductivity $\sigma = 22.9$ mS/cm (see Section 2.2.1) is

$$E = J/\sigma \approx 8.08\,\mathrm{kV/cm}. \quad (2)$$

This is in relatively good agreement with reports in the literature specifying field strengths in the ranges 6–10 kV/cm and 9–12 kV/cm as yielding 50% and 75% loss of viability, respectively, in electroporated *E. coli* [37,38]. It should be noted, however, that these literature data were reported for pulses with considerably longer durations (several ms) than the discharge in our setup, as they were all optimized for gene electrotransfer (see Section 3.2.2).

3.2.2. Gene electrotransfer into mammalian cells

Fig. 4 shows the effect of ten discharges with a peak current value of 14(±1) A, zero-to-peak time of 0.48(±0.05) μs, peak-to-halving time of 0.97(±0.06) μs, arc length of 7.0 mm, and 10(±1) ms delay between consecutive discharges, on gene transfer into CHO cells in a 60 mm culture dish. The receiving ring electrode had an outer diameter of 52 mm (fitting closely to the inner side of the dish) and an inner diameter of 46 mm.

As the figure shows, gene transfer with subsequent expression occurred at distances between approximately 3 and 15 mm from the center of the dish, while closer to the center and farther from it, no expression was detectable. From this experiment alone it is not possible to determine whether the lack of expression reflects the loss of cell viability or absence of gene transfer, but the results discussed in the preceding subsection and shown in Fig. 3 strongly suggest that in the central area the cells are irreversibly electroporated. This is also corroborated by the estimated electric field induced by radial dissipation of 14 A current through a culture medium layer with 0.90 mm thickness (1.5 ml of medium spread across a disk with a 46 mm diameter) and 14.9 mS/cm electrical conductivity, which – using the same estimation method as in the preceding section – amounts to 1.11 kV/cm and 5.54 kV/cm at 15 mm and 3 mm from the dish center, respectively. These are both roughly by a factor of 3 higher than the lowest field strengths yielding detectable gene electrotransfer and irreversible electroporation of CHO cells as obtained with pulse durations of several hundred μs to several ms – i.e., by two to three orders of magnitude longer than the discharge in our setup – that are routinely used for gene electrotransfer [39,40], for which the long "tail" of the pulse increases the efficiency due to its electrophoretic action on the DNA [41,42].

3.3. Operating considerations

3.3.1. Safety

From the safety point of view, the most important aspect is to avoid the possibility of uncontrolled discharge — either into the system operator, or other personnel or equipment nearby. For this, the discharge generator has to be disabled during its connection and disconnection to the system, as well as during the loading and unloading of the sample. Before the discharge generator is enabled, the operator has to ensure that it is connected to the system stably and reliably. In the prototype shown in Fig. 2c, the electrode connectors

are exposed, but for additional safety, connectors fully insulated from the outside can be used, yielding complete external insulation at the contact between a wire and an electrode connector.

After deciding on a generator with a given peak voltage output, wires for connection of the generator to the system have to be chosen so that their insulation is able to withstand this peak voltage with a substantial safety margin. Of the system components, the most susceptible to dielectric breakdown is the exposed part of the emitting electrode body; as explained in Section 3.1.3., it is able to withstand peak voltages at least up to 120 kV, and if the generator is capable of delivering higher voltages, the thickness of the electrode's insulation must be increased accordingly.

3.3.2. Choice of discharge generator

There are a number of power-electronic circuits able to generate an electric arc across at least several centimeters of air, the most widely commercially available being those of the self-defense electroshock weapons (tasers). Such generators allow to avoid direct contact of one electrode with the sample and deliver the current through an actual electric arc across the air separating this electrode from the sample. Such discharges also generate a distinct acoustic component, reflecting a pressure wave that accompanies the discharge, downscaled but of the same physical nature as with lightning strokes, potentially supplementing electroporation with sonoporation, and distinguishing such discharges from pulses delivered through direct contact between the electrodes and the exposed sample.

If the purpose of the setup is to study the effects of natural lightning strokes, some extent of downscaling is unavoidable, as the peak current of the most common negative strokes is ~30 kA [43]. Nonetheless, as the current of a stroke dissipates roughly radially downward and outward from its point of entry into the solid or aqueous environment, the current density and the electric field it induces are roughly inversely proportional to the square of the distance from this point. As a consequence, the conditions achieved by a stroke current with time course $I(t)$ in a given medium at 5 cm from its point of entry would also be achieved in the setup described in this article by a generator current with a time course $I(t)/100$ at 0.5 cm from its point of entry if the receiving electrode is a hemispherical bucket filled with the same medium, or at 2.5 cm if it is a ring encircling the medium 0.1 mm thick.

While the very highest current densities of lightning strokes and induced electric fields attained by lightning strokes but not attainable with downscaled exposure systems do not occur in downscaled exposure systems, those extreme conditions damage all living matter irreversibly and lethally. Moreover, they do this through rather elementary and well-understood physical and physico-chemical mechanims — heating, electrical breakdown, boiling, oxidation, etc.

Still, with electrostatic discharges triggered by dielectric breakdown, the time course of the electric current is predetermined by physics. As an example, a typical time course of the current in the most common, first negative lightning stroke (Fig. 5a), can be compared to the time course of the current in our experiment described in Section 3.2.1 (Fig. 5b). With respect to a lightning stroke (an electrostatic discharge between a cloud and the ground), the discharge generated by our setup is not only downscaled in its dimensions, current, and time, but also differs in shape — the current of a lightning stroke has a much longer falltime with respect to its risetime, and its overall time course is somewhat less regular.

The less regular time course of the current in a lightning stroke is understandable, as it propagates in stages and through different layers of air, while the longer falltime of the current in strokes largely reflects the fact that the polarization between a cloud and the ground resembles a parallel plate capacitor. In such capacitors, the charges are distributed over the plates, and upon formation of a conductive arc in the air separating them, charges first flow along the plates before entering the arc. In contrast, in our setup the charge on the emitting electrode is highly focused in its conical tip; the arc location is thus well defined and

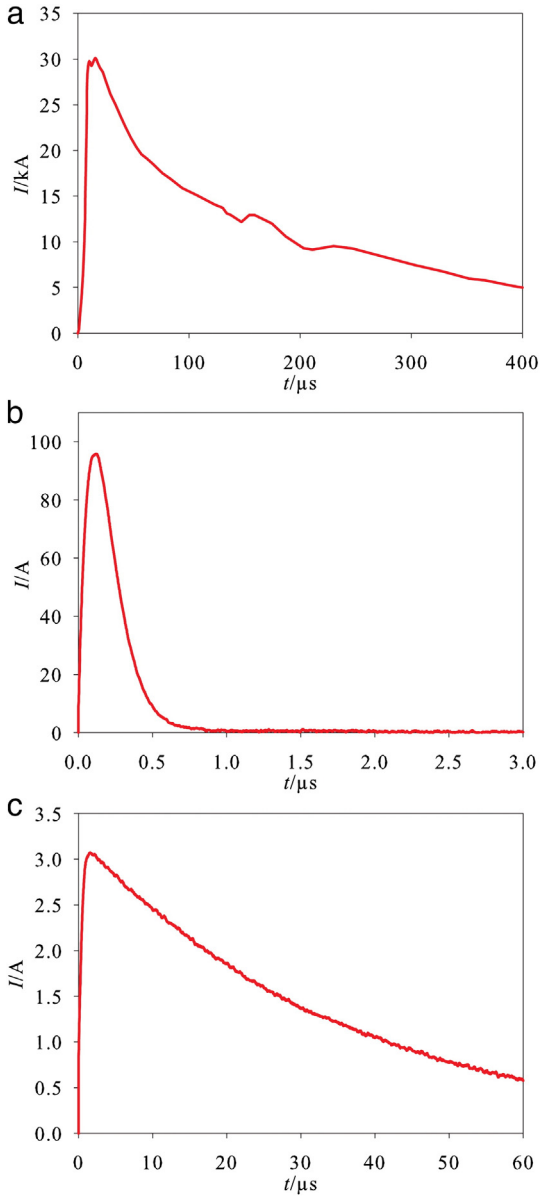

Fig. 5. Time courses of electric current, $I(t)$, from different discharge sources. (a) A natural negative first lightning stroke discharged into the ground, with the median peak current and zero-to-peak risetime as given in Table 1 of Ref. [43], and with the overall time course taken from Fig. 12 of Ref. [45]. (b) Taser gun discharged into an agar plate (details in Section 3.2.1) through a 15 mm arc. (c) A 0.25 μF capacitor discharged into an agar plate, with the emitting electrode in direct contact with the agar. Note that each of the panels features different current and time scales.

controlled, which is essential for reproducible experiments, yet reduces the time required for a complete discharge through the arc.

These differences between the time courses of the current in a stroke and its experimental model could in principle be reduced by replacing the conical emitting electrode in the experimental system by a flat one; together with the flat surface of the sample, such a setup would resemble a parallel plate capacitor. But as in all such capacitors, arcs of the discharges would then form in unpredictably varying locations, making controllable and reproducible experiments very difficult. An alternative is to avoid the arc, applying the discharge by bringing a charged parallel plate capacitor into direct electric contact with the sample. Fig. 5c shows the time course of the current generated as a 0.25 μF capacitor charged to 400 V was discharged through an agar plate as in Fig. 5b, but with the emitting electrode's tip brought into contact with the center of agar surface, and with the precharged capacitor's contacts then connected to the electrodes of the exposure system via a rapid semiconductor switch

(switching time below 0.1 μs), so that the charge did not accumulate in the electrode tip, but only passed through it. In such a setup, the time course of the current is more similar to that of a lightning stroke, with the falltime much longer than the risetime, but at the expense of further significant reduction in the magnitude of the current, which is the consequence of the limitations of a capacitor's design and maximal charging voltage it can sustain.

If one wanted to simulate also the irregularities in the typical time course of the current in strokes, the data describing such a course, suitably downscaled in magnitude, can be uploaded into a programmable function generator, its output signal then amplified by a suitable current amplifier [44] and injected into the sample similarly to the capacitor discharge described in the paragraph above. This same principle can also be applied to simulate any arbitrary current course of interest.

Acknowledgments

This work was supported by the Slovenian Research Agency (Grant P2-0249). The research was conducted in the scope of the EBAM European Associated Laboratory (LEA) and within the networking efforts of the COST Action TD1104. We would like to thank Prof. Damijan Miklavčič, head of the Department of Biomedical Engineering at our faculty, for many fruitful discussions, Dr. Saša Haberl for her advice in biological experiments, as well as Dr. Matej Reberšek and Karel Flisar for their assistance in electrical measurements.

References

[1] S.H. Davy, Elements of Chemical Philosophy: Part 1, vol. 1, Bradford and Inskeep, London, 1812.
[2] K.E. Broderick, T. Kardos, J.R. McCoy, M.P. Fons, S. Kemmerrer, N.Y. Sardesai, Piezoelectric permeabilization of mammalian dermal tissue for in vivo DNA delivery leads to enhanced protein expression and increased immunogenicity, Hum. Vaccines 7 (2011) 22–28.
[3] S. Demanèche, F. Bertolla, F. Buret, R. Nalin, A. Sailland, P. Auriol, et al., Laboratory-scale evidence for lightning-mediated gene transfer in soil, Appl. Environ. Microbiol. 67 (2001) 3440–3444.
[4] T. Kotnik, Lightning-triggered electroporation and electrofusion as possible contributors to natural horizontal gene transfer, Phys. Life Rev. 10 (2013) 351–370.
[5] T. Kotnik, Prokaryotic diversity, electrified DNA, lightning waveforms, abiotic gene transfer, and the Drake equation: assessing the hypothesis of lightning-driven evolution, Phys. Life Rev. 10 (2013) 384–388.
[6] R. Stämpfli, Reversible electrical breakdown of the excitable membrane of a Ranvier node, An. Acad. Brasil. Cienc. 30 (1958) 57–63.
[7] W.A. Hamilton, A.J.H. Sale, Effects of high electric fields on microorganisms: II. Mechanism of action of the lethal effect, Biochim. Biophys. Acta 148 (1967) 789–800.
[8] E. Neumann, K. Rosenheck, Permeability changes induced by electric impulses in vesicular membranes, J. Membr. Biol. 10 (1972) 279–290.
[9] R. Benz, F. Beckers, U. Zimmermann, Reversible electrical breakdown of lipid bilayer membranes: a charge-pulse relaxation study, J. Membr. Biol. 48 (1979) 181–204.
[10] P. Scheurich, U. Zimmermann, M. Mischel, I. Lamprecht, Membrane fusion and deformation of red blood cells by electric fields, Z. Naturforsch. 35 (1980) 1081–1085.
[11] E. Neumann, G. Gerisch, K. Opatz, Cell fusion induced by high electric impulses applied to Dictyostelium, Naturwissenschaften 67 (1980) 414–415.
[12] U. Zimmermann, P. Scheurich, High frequency fusion of plant protoplasts by electric fields, Planta 151 (1981) 26–32.
[13] U. Zimmermann, P. Scheurich, G. Pilwat, R. Benz, Cells with manipulated functions: new perspectives for cell biology, medicine, and technology, Angew. Chem. Int. Ed. 20 (1981) 325–344.
[14] B. Mali, T. Jarm, M. Snoj, G. Sersa, D. Miklavcic, Antitumor effectiveness of electrochemotherapy: a systematic review and meta-analysis, Eur. J. Surg. Oncol. 39 (2013) 4–16.
[15] T. Murakami, Y. Sunada, Plasmid DNA gene therapy by electroporation: principles and recent advances, Curr. Gene Ther. 11 (2011) 447–456.
[16] B. Rubinsky, Irreversible Electroporation, Springer Verlag, Berlin, 2010.
[17] X. Yu, P.A. McGraw, F.S. House, J.E. Crowe Jr., An optimized electrofusion-based protocol for generating virus-specific human monoclonal antibodies, J. Immunol. Methods 336 (2008) 142–151.
[18] M. Suga, T. Hatakeyama, Gene transfer and protein release of fission yeast by application of a high voltage electric pulse, Anal. Bioanal. Chem. 394 (2009) 13–16.
[19] M. Sack, J. Sigler, S. Frenzel, C. Eing, J. Arnold, T. Michelberger, et al., Research on industrial-scale electroporation devices fostering the extraction of substances from biological tissue, Food Eng. Rev. 2 (2010) 147–156.
[20] C. Gusbeth, W. Frey, H. Volkmann, T. Schwartz, H. Bluhm, Pulsed electric field treatment for bacteria reduction and its impact on hospital wastewater, Chemosphere 75 (2009) 228–233.
[21] H. Leontiadou, A.E. Mark, J. Marrink, Molecular dynamics simulations of hydrophilic pores in lipid bilayers, Biophys. J. 86 (2004) 2156–2164.
[22] M. Tarek, Membrane electroporation: a molecular dynamics simulation, Biophys. J. 88 (2005) 4045–4053.
[23] R.A. Böckmann, B.L. De Groot, S. Kakorin, E. Neumann, H. Grubmüller, Kinetics, statistics, and energetics of lipid membrane electroporation studied by molecular dynamics simulations, Biophys. J. 95 (2008) 1837–1850.
[24] V. Knecht, S.J. Marrink, Molecular dynamics simulations of lipid vesicle fusion in atomic detail, Biophys. J. 92 (2007) 4254–4261.
[25] S.J. Marrink, A.H. de Vries, D.P. Tieleman, Lipids on the move: simulations of membrane pores, domains, stalks and curves, Biochim. Biophys. Acta 1788 (2009) 149–168.
[26] E. Neumann, M. Schaefer-Ridder, Y. Wang, P.H. Hofschneider, Gene transfer into mouse lyoma cells by electroporation in high electric fields, EMBO J. 1 (1982) 841–845.
[27] H. Wolf, A. Pühler, E. Neumann, Electrotransformation of intact and osmotically sensitive cells of *Corynebacterium glutamicum*, Appl. Microbiol. Biotechnol. 30 (1989) 283–289.
[28] I.P. Sugar, Neumann, Stochastic model for electric field-induced membrane pores electroporation, Biophys. Chem. 19 (1984) 211–225.
[29] J.C. Weaver, Y.A. Chizmadzhev, Theory of electroporation: a review, Bioelectrochem. Bioenerg. 41 (1996) 135–160.
[30] T. Kotnik, G. Pucihar, D. Miklavčič, Induced transmembrane voltage and its correlation with electroporation-mediated molecular transport, J. Membr. Biol. 236 (2010) 3–13.
[31] A.E. Sowers, A long-lived fusogenic state is induced in erythrocyte ghosts by electric pulses, J. Cell Biol. 102 (1986) 1358–1362.
[32] J. Teissié, M.P. Rols, Fusion of mammalian cells in culture is obtained by creating the contact between cells after their electropermeabilization, Biochem. Biophys. Res. Commun. 140 (1986) 258–266.
[33] D.A. Stenger, S.W. Hui, Kinetics of ultrastructural changes during electrically induced fusion of human erythrocytes, J. Membr. Biol. 93 (1986) 43–53.
[34] F.S. Cohen, G.B. Melikyan, The energetics of membrane fusion from binding, through hemifusion, pore formation, and pore enlargement, J. Membr. Biol. 199 (2004) 1–14.
[35] L.V. Chernomordik, M.M. Kozlov, Mechanics of membrane fusion, Nat. Struct. Mol. Biol. 15 (2008) 675–683.
[36] I.G. Abidor, A.E. Sowers, Kinetics and mechanism of cell membrane electrofusion, Biophys. J. 61 (1992) 1557–1569.
[37] N.M. Calvin, P.C. Hanawalt, High-efficiency transformation of bacterial cells by electroporation, J. Bacteriol. 170 (1988) 2796–2801.
[38] W.J. Dower, J.F. Miller, C.W. Ragsdale, High efficiency transformation of *E.coli* by high voltage electroporation, Nucleic Acids Res. 16 (1988) 6127–6145.
[39] I. Marjanovič, S. Haberl, D. Miklavčič, M. Kandušer, M. Pavlin, Analysis and comparison of electrical pulse parameters for gene electrotransfer of two different cell lines, J. Membr. Biol. 236 (2010) 97–105.
[40] M.P. Rols, J. Teissié, Electropermeabilization of mammalian cells to macromolecules: control by pulse duration, Biophys. J. 75 (1998) 1415–1423.
[41] H. Wolf, M.P. Rols, E. Boldt, E. Neumann, J. Teissié, Control by pulse parameters of electric field-mediated gene transfer in mammalian cells, Biophys. J. 66 (1994) 524–531.
[42] M. Kanduser, D. Miklavčič, M. Pavlin, Mechanisms involved in gene electrotransfer using high- and low-voltage pulses — an in vitro study, Bioelectrochemistry 74 (2009) 265–271.
[43] P. Chowdhuri, et al., Parameters of lightning strokes: a review, IEEE Trans. Power Delivery 20 (2005) 346–358.
[44] K. Flisar, M. Puc, T. Kotnik, D. Miklavčič, Cell membrane electropermeabilization with arbitrary pulse waveforms, IEEE Eng. Med. Biol. Mag. 22 (1) (2003) 77–81.
[45] K. Berger, Parameters of lightning flashes, Electra 41 (1975) 23–37.

Igor Marjanovič was born in Jesenice, Slovenia, in 1984. He earned a B.S. in Electrical Engineering from the Faculty of Electrical Engineering, University of Ljubljana, Slovenia, in 2010. He is currently a Ph.D student at the Department of Biomedical Engineering, Faculty of Electrical Engineering, University of Ljubljana. His scientific research interests include the study of electroporation, electrofusion and gene electrotransfer of prokaryotic organisms and their relation to the horizontal gene transfer and biotic evolution.

Tadej Kotnik was born in Ljubljana, Slovenia, in 1972. He earned a Ph.D in Biophysics from University Paris XI, France, in 2000, and was awarded the Galvani Prize of the Bioelectrochemical Society in 2001. He is currently a Scientific Councilor and an Associate Professor at the Faculty of Electrical Engineering of the University of Ljubljana, Slovenia. His scientific interests include membrane electrodynamics, theoretical and experimental study of related biophysical phenomena, particularly membrane electroporation and gene electrotransfer, and computational research in number theory. He is the author of over 40 articles in SCI-ranked journals cited over 1000 times to date.